

Text: Showcasing research from the Graduate School of Engineering, Kyoto University, Japan.

Title: Highly selective phenol production from benzene on a platinum-loaded tungsten oxide photocatalyst with water and molecular oxygen: selective oxidation of water by holes for generating hydroxyl radical as the predominant source of the hydroxyl group

Particles of tungsten oxide loaded with nano-particulate platinum photocatalytically produced phenol from benzene with high selectivity in water containing molecular oxygen; the selectivity for phenol was much higher than that of conventional titanium oxide photocatalysts that generated carbon dioxide as a main product.

As featured in:



See Ryu Abe *et al.* *Catal. Sci. Technol.*, 2014, 4, 3850.



rsc.li/materials-horizons

Registered charity number: 207890

Cite this: *Catal. Sci. Technol.*, 2014, 4, 3850

Highly selective phenol production from benzene on a platinum-loaded tungsten oxide photocatalyst with water and molecular oxygen: selective oxidation of water by holes for generating hydroxyl radical as the predominant source of the hydroxyl group†

Osamu Tomita,^{ab} Bunsho Ohtani^b and Ryu Abe^{*ac}

Particles of tungsten oxide loaded with nanoparticulate platinum (Pt/WO₃) photocatalytically produced phenol from benzene with high selectivity (e.g., 74% at 69% of benzene conversion) in water containing molecular O₂; the selectivity for phenol was much higher than that on conventional titanium oxide (TiO₂) photocatalysts (both the unmodified and Pt-loaded) that generated CO₂ as a main product. Results confirmed that photoexcited electrons on the Pt/WO₃ photocatalysts mainly generated H₂O₂ from molecular O₂ through a two-electron reduction; the H₂O₂ generated did not significantly contribute to the undesirable peroxidation of the phenol produced. In contrast, the oxygen radical species, such as [•]O₂[−] or [•]HO₂, generated on TiO₂ photocatalysts partially contributed to the successive oxidation of phenol and other intermediates to reduce the selectivity for phenol. More importantly, the reactions using ¹⁸O-labeled O₂ and H₂O clearly revealed that the holes generated on Pt/WO₃ react primarily with H₂O molecules, even in the presence of benzene in aqueous solution, selectively generating [•]OH radicals that subsequently react with benzene to produce phenol. In contrast, a portion of the holes generated on TiO₂ photocatalysts reacts directly with benzene molecules, which are adsorbed on the surface of TiO₂ by strong interaction with surface hydroxyl groups. This direct oxidation of substances by holes undoubtedly enhanced non-selective oxidation, consequently lowering the selectivity for phenol by TiO₂. The two unique features of Pt/WO₃, the absence of reactive oxygen radical species from O₂ and the ability to selectively oxidize water to form [•]OH, are the most likely reasons for the highly selective phenol production.

Received 9th April 2014,
Accepted 30th April 2014

DOI: 10.1039/c4cy00445k

www.rsc.org/catalysis

1. Introduction

Chemical synthesis using semiconductor photocatalysts can be an environmentally benign process that possesses great

potential for reducing energy consumption in industrial production of useful chemicals by using light energy.^{1–3} The high reduction and oxidation potentials of photoexcited electrons and holes, respectively, generated on semiconductor particles such as TiO₂ can promote various chemical reactions, even endothermic reactions. Another advantage of photocatalytic organic synthesis is the availability of molecular oxygen (O₂) or water (H₂O) as abundant and harmless reductants or oxidants, instead of conventional, expensive reductants and oxidants that generally generate non-recyclable wastes requiring separation from the products. Molecular O₂ is an efficient electron acceptor (i.e., oxidant) for the photoexcited electron generated on TiO₂ photocatalysts, where the holes generated can directly oxidize the organic substances adsorbed and can indirectly oxidize the organic substances through formation of [•]OH radicals from H₂O molecules adsorbed on the surface; the [•]OH radicals generated subsequently oxidize the organic substances to produce the desired products.^{2,4–11} However,

^a Graduate School of Engineering, Kyoto University, Katsura, Nishikyō-ku, Kyoto 615-8510, Japan. E-mail: ryu-abe@scl.kyoto-u.ac.jp; Fax: +81 75383 2479; Tel: +81 75383 2479

^b Catalysis Research Center, Hokkaido University, Sapporo 001-0021, Japan. E-mail: ohtani@cat.hokudai.ac.jp; Fax: +81 11706 9133; Tel: +81 11706 9132

^c JSPS-NEXT Program, Koujimachi, Chiyoda-ku, Tokyo 102-0083, Japan

† Electronic supplementary information (ESI) available: Results on hydroxylation and oxidation of benzene on various photocatalysts under different conditions, such as photocatalysts loaded with different amounts of Pt cocatalysts, irradiated in aqueous solution with different pH values or different benzene concentrations, and irradiated in the copresence of benzene and 2-propanol, are shown. IR spectra of photocatalyst samples after benzene adsorption, XRD patterns and raw IR spectra of WO₃ samples prepared from tungstic acid (WO₃-TA) and the results on the hydroxylation of benzene using oxygen stable isotope on WO₃-TA are also shown. See DOI: 10.1039/c4cy00445k

TiO₂ photocatalysts generally exhibit high activity for non-selective and complete oxidation of organic compounds in the presence of ambient O₂, yielding CO₂ and highly oxidized products.^{2,12–18} This property is very useful for mineralization of toxic organic compounds but is detrimental to the development of highly selective organic synthetic systems. Only a limited number of highly selective organic syntheses using conventional TiO₂ photocatalysts in the presence of molecular O₂ have been reported.^{19,20} The low selectivity for the desired products is due to the competitive nature of successive oxidations of the products, as well as the raw materials and intermediates through undesirable pathways.^{21,22} Some oxygen radical species, such as 'O₂' or 'HO₂' generated from O₂ molecules *via* the reaction with photoexcited electrons, are thought to contribute to the oxidation of organic substances to some extent.^{23–30} Some research groups have reported highly selective organic synthesis using TiO₂-related photocatalysts in the absence of molecular O₂.^{31–34} For example, Shiraishi *et al.* demonstrated highly selective synthesis of benzimidazoles from *ortho*-phenylenediamine and ethanol using a Pt-loaded TiO₂ photocatalyst (Pt/TiO₂) under UV light irradiation.³¹ Yoshida *et al.* reported direct hydroxylation of benzenes to phenols using Pt/TiO₂ suspended in water containing a high concentration of substances such as benzene (*e.g.*, 1:1 v/v), in which selectivity for hydroxylation of benzenes was greatly improved because the reaction was conducted in the absence of molecular O₂.³² In these reactions on Pt/TiO₂ photocatalysts, protons (H⁺) were used as an electron acceptor instead of molecular O₂, accompanied by production of H₂ on Pt cocatalysts. Although these reports might indicate the potential of highly selective organic synthesis through the use of photocatalysts, reaction efficiencies generally decreased significantly due to the reduced ability of H⁺ as an electron acceptor compared to O₂. Furthermore, the potential of H⁺ reduction requires a highly negative conduction band minimum (CBM) of the semiconductor and therefore limits the applicable semiconductor materials to TiO₂. The use of TiO₂ photocatalysts is limited in practical applications by their wide bandgaps (*ca.* 3.2 eV for anatase, *ca.* 3.0 eV for rutile) that require UV light irradiation for excitation. The energy efficiencies in artificial UV light sources, such as high-pressure Hg lamps or UV-LEDs, are low and insufficient for achieving cost-effective chemical synthesis using TiO₂ photocatalysts. Thus, using visible light is desired for the lower cost provided by efficient visible light sources such as blue-LEDs as well as for the possibility of using natural sunlight.

Previous studies have demonstrated that particles of tungsten oxide (WO₃) loaded with nanoparticulate platinum (Pt) exhibit photocatalytic activity sufficient for oxidation of various organic compounds under visible light; the activity was similar to that of TiO₂ under UV light.³⁵ Although WO₃ generally has been regarded as a photocatalyst inactive for oxidation of organic compounds with molecular O₂ due to an insufficient CBM for reduction of O₂, the loading of the nanoparticulate Pt cocatalyst significantly increases the probability of multi-electron reduction of O₂ by photoexcited electrons,

enhancing the oxidation of organic substances by the holes remaining in the valence band. The photoexcited electrons in Pt-loaded WO₃ (Pt/WO₃) have been suggested to produce mainly H₂O₂ *via* two-electron reduction. These findings have led to the application of the Pt/WO₃ photocatalyst to organic synthesis reactions because it is activated under visible light but does not generate oxygen radicals such as 'O₂' or 'HO₂', which may enhance the peroxidation of products. The direct hydroxylation of benzene to phenol has been selected as the target reaction because it is one of the most challenging chemical reactions. The present industrial synthesis of phenol, the major source of phenol resins, is based on the cumene method—a multi-step process that requires a large amount of energy. Therefore, direct one-step synthesis of phenol from benzene is a desirable process and has been studied extensively. The Pt/WO₃ photocatalysts have recently been shown to possess activity for direct production of phenol from benzene using O₂ and water as reactants under UV or visible light.³⁶ Selectivity for phenol on Pt/WO₃ photocatalysts was much greater than that on Pt/TiO₂ (or unmodified TiO₂) photocatalysts; however, the reasons for the differences in reactivity and selectivity of the two photocatalysis systems are not known.

The present study examined the reaction mechanism of highly selective phenol production from benzene on Pt/WO₃ photocatalysts in detail compared to that on TiO₂ (including Pt-loaded TiO₂) to find the contributing factors. Results revealed that the holes generated in the WO₃ photocatalysts possess distinctly different reactivity from those in TiO₂ toward oxidation and hydroxylation of benzene, regardless of their similar oxidation potentials, enabling highly selective phenol production from benzene in water.

2. Experimental section

2.1. Samples

Commercially available WO₃ powders, such as WO₃-K (triclinic and monoclinic, 4.8 m² g⁻¹, Kojundo Chemical Laboratory), WO₃-Y (monoclinic, 2.2 m² g⁻¹, Yamanaka Chemical Industries), and WO₃-S (monoclinic, 1.6 m² g⁻¹, Soekawa Chemicals), were used. The fine particulate WO₃ sample, referred to as WO₃-K (triclinic, 10 m² g⁻¹), was obtained by separation from large aggregates by means of centrifugation of the purchased WO₃-K samples as previously reported.³⁵ The TiO₂ powders, such as TiO₂-P [anatase and rutile, P 25, 55 m² g⁻¹, Degussa (Evonik)], TiO₂-A (anatase, 10 m² g⁻¹, Merck), and TiO₂-R (rutile, 4.0 m² g⁻¹, Aldrich), were used.

2.2. Platinum loading using the photodeposition method

Samples loaded with Pt nanoparticles were prepared as follows. The sample powder was stirred in an aqueous methanol solution (10 vol%) containing the required amount of H₂PtCl₆ as the Pt precursor. The WO₃ samples were irradiated with visible light; the TiO₂ samples were irradiated with UV and visible light. After washing several times with distilled water, the sample was dried in air at 353 K for 12 h. The diameters

of the loaded Pt nanoparticles were confirmed to be 3–10 nm as demonstrated in the previous study.³⁵

2.3. Photocatalytic reaction

The photocatalytic reaction of benzene was conducted in a Pyrex reaction cell (15 mL) in an aerated aqueous benzene solution (water volume: 7.5 mL; initial benzene amount: 18.8 μmol) with continuous stirring at 279 K. The source for both the ultraviolet and visible light was a 300 W xenon lamp so that results could be compared with those of TiO_2 photocatalysts ($300 < \lambda < 500 \text{ nm}$). Sample aliquots were withdrawn from the reactor cell after each irradiation and filtered through a PVDF filter (Mini-Uni Prep™) to remove the photocatalyst particles. Product analysis was performed using a high performance liquid chromatograph equipped with a C-18 column and a photodiode-array detector (Shimadzu, SPD-M20A). The generation of carbon dioxide in the gas phase was analyzed using a gas chromatograph (Shimadzu, GC-14B) equipped with a flame-ionization detector.

The amount of H_2O_2 produced during photocatalytic oxidation of an organic substrate was analyzed by iodometry.³⁷ The photocatalyst (10 mg) suspended in 10 mL of water was placed in a Pyrex test tube (30 mL) in the presence of ambient oxygen. The initial amount of acetic acid (as the hole scavenger) was 300 μmol . After irradiation of the photocatalyst suspension, 2 mL of the solution was removed with a syringe and the photocatalyst separated from the solution using a syringe PVDF filter (Millex®W). Then 1 mL of 100 mmol L^{-1} aq. potassium hydrogen phthalate ($\text{C}_8\text{H}_5\text{KO}_4$) and 1 mL of 400 mmol L^{-1} aq. potassium iodide (KI) were added. H_2O_2 was allowed to react with I^- under acidic conditions ($\text{H}_2\text{O}_2 + 3\text{I}^- + 2\text{H}^+ \rightarrow \text{I}_3^- + 2\text{H}_2\text{O}$). The amount of H_2O_2 was determined by the maximum intensity of absorption attributed to I_3^- at approximately 350 nm, measured using a UV-Vis spectrophotometer (Shimadzu UV-1800).

For tracer studies, either H_2^{18}O (98 atom%, Taiyo Nippon Sanso Corp.) or $^{18}\text{O}_2$ (98 atom%, Taiyo Nippon Sanso Corp.) gas was used as the oxygen isotope source. Then, 50 mg of the photocatalyst suspended in 1 mL of H_2^{18}O (in air) or H_2^{16}O (in $^{18}\text{O}_2$) was used. In the case of reactions in the H_2^{16}O solvent with $^{18}\text{O}_2$ gas, the solution was purged with Ar gas and subsequently with $^{18}\text{O}_2$ gas to make the partial pressure of O_2 in the reaction system similar to that in air; the amount of N_2 gas was under the detection limit in each reaction. The initial amount of benzene used to investigate the hydroxylation process of benzene to phenol was 500 μmol (500 mmol L^{-1}). After the photocatalyst suspended in solution had been irradiated, a portion (20 μL) was extracted by a syringe, added to diethyl ether (300 μL) containing the internal standard, and shaken in a tube mixer. The amount of ^{18}O -labeled phenol was determined using GC-MS (Shimadzu, GCMS-2010/PARVUM2).

2.4. IR measurements

The FT-IR spectra of the adsorbed benzene on each sample were recorded with a Fourier-transform infrared spectrometer

(Jasco FT-4200). The sample pellet was introduced into an IR cell equipped with CaF_2 windows. Prior to the measurements, the sample was heated in vacuum. After cooling, benzene vapor was introduced into the cell and then evacuated in the gas phase. The spectra obtained after adsorption of benzene were subtracted from the corresponding spectra before adsorption.

3. Results and discussion

3.1. Hydroxylation of benzene over various Pt/ WO_3 and Pt/ TiO_2 photocatalysts

Fig. 1 shows the time course of photocatalytic hydroxylation and oxidation of benzene on Pt-loaded WO_3 and Pt-loaded TiO_2 samples in water (7.5 mL) containing saturated air and a small amount of benzene (*ca.* 18.8 μmol). Reactions were started with the benzene concentration (2.5 mmol L^{-1}) sufficiently lower than the maximum soluble value of benzene in water (22.3 mmol L^{-1}), in order to accurately quantify the reduced amount of benzene during each reaction.³⁸ Upon irradiation with UV and visible light, the amount of benzene decreased, while the rate and the order of reaction varied among the samples. Selectivity for each product was distinctly different for the Pt/ WO_3 and Pt/ TiO_2 systems.

Phenol and CO_2 were the predominant products in the Pt/ WO_3 and Pt/ TiO_2 systems, respectively. For Pt/ WO_3 -K (Fig. 1a), phenol was produced at an almost steady rate under irradiation along with small amounts of di-hydroxylated benzenes (not plotted) and CO_2 .

Table 1 summarizes the selectivity for each product, calculated on the basis of the decrease in benzene. Because selectivity for CO_2 is difficult to determine due to uncertainty in the stoichiometry between the decrease in benzene and the generation of CO_2 , the amount of CO_2 generated is listed in Table 1. Selectivity for phenol by the Pt/ WO_3 -K photocatalyst (entry 1) initially (1 h) was *ca.* 79%, with a benzene conversion of 22%, along with appreciable production of catechol (1.9%), hydroquinone (1.2%), and *p*-benzoquinone (4.0%). The generation of CO_2 was below the detection limit ($<0.1 \mu\text{mol}$).

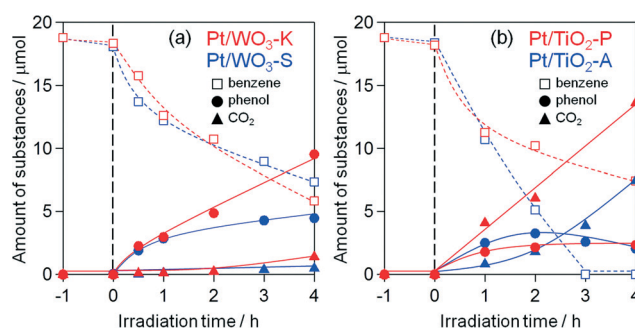


Fig. 1 Time course curves of photocatalytic oxidation of benzene over (a) Pt/ WO_3 and (b) Pt/ TiO_2 photocatalysts in aerated aqueous solutions of benzene (18.8 μmol) under ultraviolet and visible light irradiation ($300 < \lambda < 500 \text{ nm}$).

Table 1 Conversion and phenol selectivity of hydroxylation of benzene^a

Entry	Photocatalyst	Conversion ^b (%)	Selectivity ^c (%)					Amount of CO ₂ /μmol
			phenol	Catechol	Resorcinol	Hydroquinone	Benzoquinone	
1	Pt/WO ₃ -K	22.2 (1)	79.3	1.9	0	1.2	4.0	<0.1
		68.9 (4)	73.7	2.3	0.7	0	8.8	1.4
2	Pt/WO ₃ -Y	40.6 (4)	58.8	1.2	0	1.3	1.1	<0.1
		63.6 (4)	57.1	1.4	0	2.2	0.5	0.4
3	Pt/WO ₃ -S	32.4 (1)	48.7	1.2	0	2.0	1.2	0.6
		59.2 (4)	41.7	1.2	0	2.1	0.0	1.1
4	WO ₃ -K	16.4 (4)	84.6	1.6	0	3.3	1.1	<0.1
5 ^d	Pt/TiO ₂ -P	26.6 (1)	83.8	1.4	0	1.2	2.8	<0.1
		52.5 (4)	75.1	1.4	0	2.9	1.2	0.6
6	Pt/TiO ₂ -P	38.0 (1)	25.9	0	0	0.6	1.1	4.1
		59.1 (4)	21.8	0	<0.1	0.8	0.1	13.6
7	Pt/TiO ₂ -A	43.0 (1)	31.0	2.8	0	1.9	0	0.8
		99.0 (4)	10.9	4.2	0.3	2.1	0	7.5
8	Pt/TiO ₂ -R	24.1 (1)	36.9	3.2	0	9.1	1.7	1.5
		76.8 (4)	11.9	2.6	0.1	5.9	1.7	3.7
9	TiO ₂ -P	51.6 (1)	22.7	0	0	1.4	0.2	4.7
		82.5 (4)	20.8	<0.1	0	0.8	0.1	13.4
10	TiO ₂ -A	37.8 (1)	23.6	3.4	0	3.0	0	0.4
		84.5 (4)	14.5	5.7	0.1	2.8	0	4.9
11	TiO ₂ -R	34.1 (1)	24.8	1.6	0	11.5	0	1.8
		68.3 (4)	16.1	1.6	0	6.7	0	12.5

^a Initial amount of benzene: 18.8 μmol, solvent: H₂O 7.5 mL, light source: 300 W Xe lamp. ^b Conversion: $(C_{\text{benzene},0} - C_{\text{benzene},t})/C_{\text{benzene},0} \times 10^2$.

^c Selectivity: $C_{\text{products},t}/(C_{\text{benzene},0} - C_{\text{benzene},t}) \times 10^2$. ^d Under visible light irradiation (400 < λ < 500 nm).

Even with high benzene conversion (68.9%) after a long period of irradiation (4 h), selectivity for phenol was high (74%), while the amount of CO₂ became detectable (*ca.* 1.4 μmol). The Pt/WO₃-K photocatalyst had high selectivity for hydroxylated benzene or quinone throughout the reaction period (*ca.* 86.4% and 85.5% after 1 and 4 h of irradiation, respectively). The products without an aromatic ring were not quantified because quantification by HPLC was difficult, even with a photodiode array detector. Therefore, the unidentified fraction (*ca.* 14%) reflected the cleaved intermediates, including oxidized CO₂. Other Pt/WO₃ samples also generated phenol as the main product with relatively high selectivity and a negligibly small amount of CO₂ (Fig. 1a and S1a,† and Table 1) in the initial period (1 h), while the Pt/WO₃-S sample showed significantly lower selectivity (*ca.* 42%) after 4 h of irradiation. These findings strongly suggest that the rate of successive oxidation of phenol on Pt/WO₃ photocatalysts, specifically on the Pt/WO₃-K sample, is lower than that of hydroxylation of benzene, affording high selectivity for phenol.

In contrast, CO₂ was predominantly generated on Pt/TiO₂-P (Fig. 1b) at a steady rate during the initial period along with an appreciable amount of phenol. The amount of phenol nearly reached saturation after 1 h of photo-irradiation, indicating successive oxidation of the phenol once produced to give cleaved intermediates and CO₂. The production of CO₂ during the initial period strongly suggests a direct oxidation pathway of benzene without the formation of any hydroxylated intermediates such as phenol. Selectivity for phenol was quite low (*ca.* 26%) on Pt/TiO₂-P, even at short irradiation times (1 h) with relatively low conversion of benzene (Table 1, entry 6). The use of other Pt/TiO₂ samples also resulted in

predominant production of CO₂, along with much lower selectivity for phenol (Fig. 1b and S1,† Table 1) than that of Pt/WO₃. However, the time courses for CO₂ and phenol production were different from those using Pt/TiO₂-P. For example, the use of Pt/TiO₂-A (Fig. 1b) generated predominantly phenol during the initial period, followed by the generation of CO₂ along with a gradual decrease in the phenol amount, indicating successive oxidation of the phenol produced. Similar reactivity was observed for the Pt/TiO₂-R sample with the pure rutile phase (Fig. S1†). Selectivity for phenol on these Pt/TiO₂ photocatalysts (Table 1, entries 6–8) was much lower than that on the Pt/WO₃ photocatalysts. Note that the Pt/WO₃-K and the Pt/TiO₂-A samples, which have similar surface areas (*ca.* 10 m² g⁻¹), possessed different reactivities. Thus, the factor dominating reactivity is related to the difference in the composition (WO₃ or TiO₂), not on the surface area.

These results indicate that the rates of successive oxidation of phenol on Pt/WO₃ photocatalysts are much lower than those on Pt/TiO₂ photocatalysts, enabling Pt/WO₃ to produce phenol with high selectivity. Another advantage of Pt/WO₃ photocatalysts is their ability to be used under visible light irradiation. As shown in Table 1, visible light irradiation (λ > 400 nm) afforded better phenol selectivity (entry 5) than did full arc irradiation (entry 1) on the Pt/WO₃-K photocatalyst, with a comparable reaction rate. For Pt/TiO₂-P with mixed anatase and rutile phases, an appreciable decrease in benzene amount was observed (Fig. S2†) certainly due to the reaction on the rutile phase that can absorb light up to *ca.* 410 nm, while the rate was much lower than that under UV light irradiation (Fig. 1). As expected based on the photoabsorption properties of TiO₂ anatase, visible light

irradiation of Pt/TiO₂-A did not yield any appreciable products (Fig. S2†).

3.2. Influence of oxygen-reduced species on phenol selectivity by Pt/WO₃ and Pt/TiO₂ photocatalysts

The Pt/WO₃ photocatalysts exhibited significantly greater selectivity for phenol production than did the Pt/TiO₂ system, which showed high activity for oxidative degradation of benzene and other intermediates including phenols. A possible reason for the difference in reactivity between the two systems could be a difference in the level of participation of the O₂ reduced species (H₂O₂, 'O₂⁻, or 'HO₂), generated during the reductive process by photoexcited electrons, in the oxidation of benzene or intermediates. The conduction band minimum (CBM) of the WO₃ semiconductor (*ca.* +0.5 V *vs.* SHE) was much lower than the potentials of O₂ reduction *via* the one-electron process [O₂ + e⁻ → 'O₂⁻, E⁰(O₂/'O₂⁻) = -0.28 V; or O₂ + H⁺ + e⁻ → 'HO₂, E⁰(O₂/'HO₂) = -0.05 V *vs.* SHE], resulting in rapid recombination between photoexcited electrons and holes in WO₃ photocatalysts even in the presence of a sufficient amount of O₂. Unmodified WO₃ samples indeed exhibited a low rate of benzene oxidation and hydroxylation, but the selectivity for phenol was adequate (Table 1, entry 4). However, loading of highly dispersed Pt nanoparticles on WO₃ was shown to significantly enhance the rate of oxidative decomposition of aliphatic compounds, such as acetaldehyde, under visible light. This enhancement is due to the promotion of multi-electron reduction of O₂ [O₂ + 2e⁻ + 2H⁺ → H₂O₂, E⁰(O₂/H₂O₂) = +0.68 V; or O₂ + 4e⁻ + 4H⁺ → 2H₂O, E⁰(O₂/H₂O) = +1.23 V *vs.* SHE] on Pt cocatalysts; these reactions are able to proceed thermodynamically, even through the photoexcited electrons generated in the conduction band of WO₃. The small amount of Pt loading (0.1 wt.%) was also effective for enhancing the rate of hydroxylation and oxidation of benzene on Pt/WO₃-K photocatalysts, strongly suggesting the occurrence of multi-electron reduction of O₂ on the Pt cocatalyst in the present system. As shown in Fig. S3†, the optimum amount of Pt loading for phenol production was *ca.* 0.1 wt.%; greater amounts resulted in lower selectivity for phenol and increased the generation of CO₂, while the reaction rate was increased.

In contrast, TiO₂ semiconductors possess a much more negative CBM (anatase: *ca.* -0.2 V, rutile: *ca.* +0.05 V *vs.* SHE) than that of WO₃. These values, especially those of anatase, are considered sufficient for the progress of O₂ reduction *via* a single-electron process by assuming a shift in the CBM potentials of TiO₂ under near neutral pH conditions.³⁹ Most TiO₂ photocatalysts, especially those with anatase, exhibit sufficiently high activity for oxidative degradation of various organic compounds even without a cocatalyst such as Pt. In the present system, the unmodified TiO₂-P photocatalyst exhibited greater conversion of benzene than that loaded with 0.1 wt.% of Pt (see Table 1 and Fig. S3†), implying that most of the photoexcited electrons were consumed on the TiO₂ surface, even with Pt loading, *via* single-electron processes

producing radical species of O₂ (*e.g.*, 'O₂⁻ or 'HO₂). As shown in Fig. S3†, selectivity for phenol on TiO₂ photocatalysts was minimally affected by the Pt loading amount, while the conversion of benzene on Pt/TiO₂-A increased significantly with the Pt loading amount. Thus, an amount of 0.1 wt.% Pt loading in the TiO₂ system is a reasonable value for comparison with the Pt/WO₃ system.

Products generated from molecular O₂ during the reduction on WO₃ and TiO₂ were evaluated using the photocatalytic oxidation of acetic acid in aqueous solution containing O₂. Fig. 2 shows the time courses for H₂O₂ and CO₂ production over WO₃ and TiO₂ photocatalysts suspended in aqueous acetic acid (AcOH) under both ultraviolet and visible light irradiation (300 < λ < 500 nm). (Time courses for other samples are shown in Fig. S4†) Under irradiation, both H₂O₂ and CO₂ were simultaneously generated on unmodified and Pt-loaded WO₃ samples, while the rates were much greater with the Pt-loaded samples. Saturation of H₂O₂ on Pt/WO₃ samples was undoubtedly due to the catalytic decomposition of H₂O₂ into H₂O and O₂ on Pt particles, with a possible contribution of photocatalysis by electrons or holes. Assuming that CO₂ generation occurred only by photogenerated holes (CH₃COOH + 2H₂O + 8H⁺ → 2CO₂ + 8H⁺), combining this process with H₂O₂ generation (O₂ + 2H⁺ + 2e⁻ → H₂O₂) should result in the generation of H₂O₂ and CO₂ with an ideal stoichiometric ratio of 2 : 1 (CH₃COOH + 2H₂O + 4O₂ → 4H₂O₂ + 2CO₂). As summarized in Table 2, the ratio of the amount of H₂O₂ generated to that of CO₂ was close to the stoichiometric value, both on unmodified and Pt-loaded WO₃-K samples (2.4 and 2.1), indicating that most of the photoexcited electrons on WO₃-K were consumed *via* the two-electron reduction of O₂, producing H₂O₂. Other Pt/WO₃ samples also showed appreciable generation of H₂O₂ with CO₂, while the rates of H₂O₂ production were lower than the stoichiometric value expected from the CO₂ generation. This deviation is likely due to the catalytic and/or photocatalytic decomposition of H₂O₂ and possibly the four-electron reduction of O₂ to H₂O on the Pt cocatalyst.

In contrast, the generation of H₂O₂ on TiO₂-P was negligibly low, independent of Pt loading, despite the high rates of CO₂ generation (Fig. 2 and Table 2, entries 4 and 8). These results indicate that the photoexcited electrons on the TiO₂-P photocatalyst were consumed mainly *via* one-electron processes

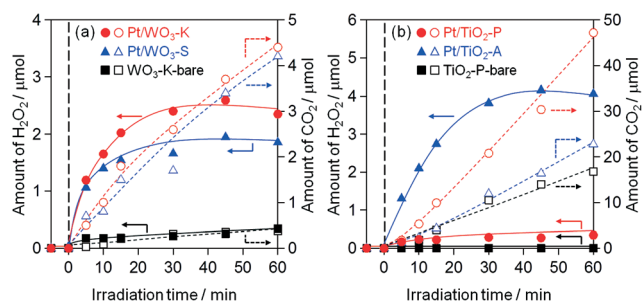


Fig. 2 Time course curves of H₂O₂ and CO₂ generation over (a) WO₃ and (b) TiO₂ photocatalysts suspended in AcOH solution under ultraviolet and visible light irradiation (300 < λ < 500 nm).

Table 2 Initial production rate of H₂O₂ and CO₂ over WO₃ and TiO₂ photocatalysts suspended in aq. AcOH^a

Entry	Photocatalyst	Amount of H ₂ O ₂ production/ μ mol	Amount of CO ₂ production/ μ mol	Ratio of amount of H ₂ O ₂ to CO ₂
1	Pt/WO ₃ -K	1.2	0.5	2.4
2	Pt/WO ₃ -Y	1.1	0.7	1.4
3	Pt/WO ₃ -S	0.6	0.5	1.1
4	Pt/TiO ₂ -P	0.2	1.8	0.1
5	Pt/TiO ₂ -A	1.3	1.2	1.1
6 ^b	Pt/TiO ₂ -R	0.9	1.0	0.9
7 ^b	WO ₃ -K	0.2	0.1	2.1
8	TiO ₂ -P	0	1.2	0
9	TiO ₂ -A	0.2	0.7	0.3
10 ^b	TiO ₂ -R	0.1	0.1	1.2

^a Initial amount of AcOH: 300 μ mol, amount of solvent (H₂O): 10 mL, light source: 300 W Xe lamp (300 < λ < 500 nm); calculated on the amount of products after 5 min. ^b Calculated on the amount of products after 10 min.

producing radical species (O_2^- or HO_2), although four-electron reduction of O₂ to form H₂O on the Pt-loaded sample was also possible. On other TiO₂-A and TiO₂-R samples, H₂O₂ generation was appreciable, especially after Pt loading, indicating enhanced two-electron reduction of O₂ on the Pt cocatalyst.

Comparison of the results shown in Tables 1 and 2 indicates a connection between the selectivity for H₂O₂ generation from aq. AcOH and the selectivity for phenol from benzene. The TiO₂ samples with low selectivity for H₂O₂ production (*e.g.*, unmodified TiO₂-P, Pt/TiO₂-P) that indicated high selectivity for oxygen radical species (O_2^- or HO_2) tended to exhibit low selectivity for phenol production from benzene. However, samples with high selectivity for H₂O₂ generation (*e.g.*, Pt/TiO₂-A, Pt/TiO₂-R) exhibited appreciably higher selectivity for phenol. These findings suggest that the oxygen radical species (O_2^- or HO_2) generated on TiO₂ samples contributed to oxidative decomposition of the substrates and consequently lowered selectivity for phenol. Although the contribution of these oxygen radical species toward oxidation of organic compounds is not well understood, the oxidative reactivity of the radical species (O_2^- or HO_2) should be greater than that of non-radical H₂O₂. Some studies have

suggested that the O_2^- species generated during photocatalysis on TiO₂ enhanced the cleavage of aromatic rings.³⁰ However, the generation of reactive oxygen radical species is suppressed in the Pt/WO₃ systems by the lower CBM, which forces reduction of O₂ molecules into H₂O₂ or H₂O *via* a multi-electron process.

These results have prompted the hypothesis that the high selectivity for phenol on Pt/WO₃ is due to the absence of reactive oxygen radical species (O_2^- or HO_2), which enhances oxidative decomposition of the phenol or other intermediates produced. This hypothesis is supported by the results from photocatalytic oxidation and hydroxylation of benzene in the absence of molecular O₂, which are summarized in Table 3. For the Pt/WO₃ system, reactions were conducted in the presence of Ag⁺ as an electron acceptor instead of O₂, because it possesses an appropriate potential [+0.799 V *vs.* SHE] for efficient scavenging of photoexcited electrons generated in WO₃. Since the addition of AgNO₃ (18.8 μ mol) makes the aqueous solution acidic (pH \sim 5), the influence of pH on phenol selectivity needs to be considered. Phenol selectivity of the Pt/WO₃-K samples was reduced by decreasing pH value (Fig. S5[†]). Therefore, results for the Pt/WO₃-K samples in the presence of O₂

Table 3 Hydroxylation of benzene over WO₃ photocatalysts in the absence of molecular O₂^a

Entry	Reaction conditions	Photocatalyst	Conversion (%) (irradiation time/h)	Phenol selectivity (%)
Ref. 1	O ₂ pH \sim 6	Pt/WO ₃ -K	22.2 (1)	79.3
Ref. 2	O ₂ pH \sim 5	Pt/WO ₃ -K	18.9 (1)	55.4
1	Ag ⁺ , Ar	Pt/WO ₃ -K	27.5 (1)	54.0
			53.0 (3)	51.5
2	Ag ⁺ , Ar	Pt/WO ₃ -Y	40.8 (1)	50.1
			72.3 (3)	50.3
3	Ag ⁺ , Ar	Pt/WO ₃ -S	46.9 (1)	48.2
			71.1 (3)	51.5
4	H ⁺ , Ar	Pt/TiO ₂ -P	13.3 (1)	60.8
			33.8 (4)	34.0
5	H ⁺ , Ar	Pt/TiO ₂ -A	10.8 (0.3)	51.9
			27.4 (4)	26.1
6	H ⁺ , Ar	Pt/TiO ₂ -R	11.6 (1)	41.8
			25.8 (4)	27.2
7	H ⁺ , Ar	TiO ₂ -P-bare	19.8 (0.5)	50.5

^a Initial amount of benzene: 18.8 μ mol, initial amount of Ag⁺ ion: 18.8 μ mol, amount of solvent (H₂O): 7.5 mL, light source: 300 W Xe lamp (300 < λ < 500 nm).

(i.e., in the absence of Ag^+) at different pH values are included in Table 3 for comparison.

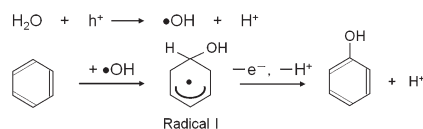
Interestingly, selectivity for phenol by the Pt/WO_3 system was minimally affected by the presence of O_2 ; similar values for phenol selectivity were obtained with or without O_2 , even at different reaction times (i.e., at different levels of benzene conversion). These findings strongly suggest that the H_2O_2 generated by the Pt/WO_3 system *via* reduction of O_2 did not significantly contribute to the undesirable peroxidation of phenol. These results also imply that the existence of O_2 in the reaction media, whether it is reduced or not, has no impact on phenol selectivity. In contrast, the existence of O_2 significantly decreased selectivity for phenol in the Pt/TiO_2 system. For the Pt/TiO_2 system, reactions were initiated in deaerated water containing only benzene, without adding any electron acceptor, because the CBM of TiO_2 , especially that of anatase, is sufficient for reduction of water (or H^+) to H_2 (generation of H_2 was confirmed for all of the Pt/TiO_2 samples). As summarized in Table 3, selectivity for phenol by the Pt/TiO_2 samples improved significantly by conducting the reactions in the absence of O_2 , while the conversions at the same reaction time decreased compared to those with O_2 (see Table 1) primarily due to the lower reaction rate of photoexcited electrons with H^+ than that with O_2 . For example, phenol selectivity on $\text{Pt}/\text{TiO}_2\text{-P}$ was improved significantly from 26 to 61% during the initial period (Table 1, entry 6; Table 3, entry 4). Yoshida *et al.* also demonstrated improved phenol selectivity using Pt/TiO_2 photocatalysts in a deaerated solution of benzene and water (1:1 by vol.).³² The same tendency was observed on unmodified $\text{TiO}_2\text{-P}$ in the presence of an Ag^+ electron acceptor (Table 3, entry 7); selectivity for phenol was improved from *ca.* 23% (Table 1, entry 9) to 50% at 30 min of reaction by removing O_2 from the solution. These findings strongly support the hypothesis that the oxygen radical species (O_2^- or HO_2^\cdot) generated on TiO_2 contributed to oxidative decomposition of the substrate including phenol, consequently lowering selectivity for phenol. However, selectivity for phenol in the Pt/TiO_2 system decreased significantly upon prolonged reaction time, even in the absence of O_2 (Table 3, entries 4–6), in contrast to results in the Pt/WO_3 system. These results suggest that factors other than the reactive oxygen radical species contribute to the difference in reactivity between Pt/WO_3 and Pt/TiO_2 (including unmodified TiO_2) for hydroxylation and oxidation of benzene. The most likely cause is the difference in reactivity of the holes generated in each photocatalyst system. To clarify the reasons for the reactivity differences, specifically the difference in selectivity of holes for phenol production on the WO_3 and TiO_2 systems, the reaction mechanism for each system was investigated in detail using ^{18}O -labeled O_2 and H_2O .

3.3. Determination of oxygen sources for phenol production from benzene on Pt/WO_3 and Pt/TiO_2 systems using ^{18}O -labeled O_2 and H_2O

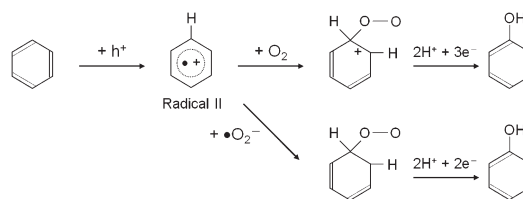
In general, the photocatalytic hydroxylation of benzene to phenols is considered to proceed through two different routes

as illustrated in Schemes 1 and 2.^{2,40–44} The first route (Scheme 1) is initiated by photocatalytic generation of hydroxyl radicals (OH^\cdot) from H_2O molecules and/or surface hydroxyl groups of the semiconductor, which then react with benzene molecules to yield benzene radical species (radical I). The benzene radical species then reacts with another OH^\cdot in solution or a hole on the semiconductor to produce phenol. If phenol production proceeds through this route, the O atoms originally contained in the H_2O molecules of the solvent must be introduced into the phenol. The route shown in Scheme 2, which has been suggested recently by Matsumura *et al.*,⁴³ is initiated by direct oxidation of benzene molecules on the semiconductor surface with photo-generated holes, giving cationic radical species of benzene (radical II). The cationic radical species are then attacked by O_2 or O_2^- molecules to give peroxidized species. The peroxidized species are then transformed into phenol molecules accompanied by proton (H^+)-coupled reduction with photoexcited electrons (e^-), as shown in Scheme 2. In this case, the phenol molecules produced must contain O atoms originating from the molecular O_2 dissolved in the solution. To clarify the dominant route operating in phenol production on Pt/WO_3 and Pt/TiO_2 systems, reactions were conducted using a stable oxygen isotope (^{18}O -enriched water: H_2^{18}O or $^{18}\text{O}_2$).

Fig. 3 and S7† show time courses for production of phenol from benzene by photocatalysis using four Pt/WO_3 and Pt/TiO_2 samples, conducted in ^{18}O -enriched water (1.0 mL, 98% H_2^{18}O) containing benzene and molecular O_2 ($^{16}\text{O}_2$). The total amount of phenol produced and the percentage of phenol containing ^{18}O were plotted against irradiation time. A larger amount of benzene (500 μmol) was added to water for these reactions compared to that for reactions shown in Fig. 1 to minimize successive peroxidation of phenol. Photoirradiation of $\text{Pt}/\text{WO}_3\text{-K}$ produced phenol at a nearly steady rate; the percentage of ^{18}O -labeled phenol was greater than 90% throughout the reaction, while the percentage decreased slightly from 95% (15 min) to 91% (8 h) during the reaction (Table 4, entry 1). The high percentage of ^{18}O -labeled phenol



Scheme 1 Proposed reaction for phenol production over photocatalysts *via* hydroxyl radical.



Scheme 2 Proposed reaction for phenol production over photocatalysts *via* oxygen molecule and oxygen radical.

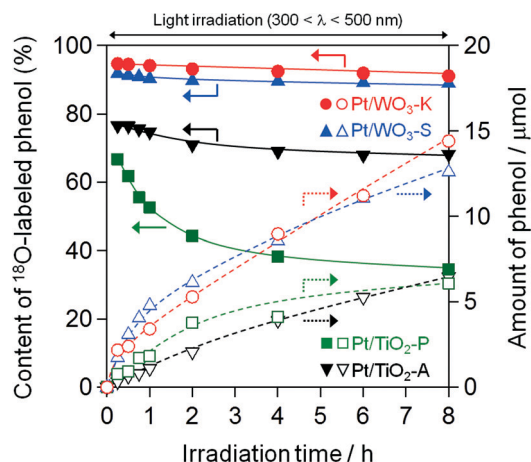


Fig. 3 Time course curves of photocatalyzed production of phenol from benzene on Pt/WO_3 and Pt/TiO_2 samples. Reactions were conducted in ^{18}O -enriched water (98% H_2^{18}O) containing benzene and normal molecular $^{16}\text{O}_2$.

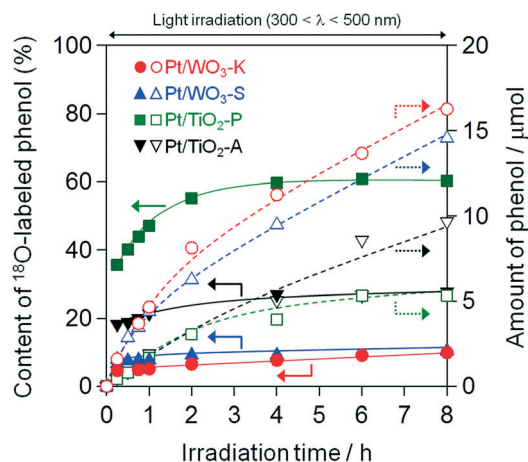


Fig. 4 Time course curves of photocatalyzed production of phenol from benzene on Pt/WO_3 and Pt/TiO_2 samples. Reactions were conducted in normal water (H_2^{16}O) containing benzene and molecular $^{18}\text{O}_2$.

throughout the reaction indicated that phenol production on $\text{Pt}/\text{WO}_3\text{-K}$ proceeded primarily *via* a reaction pathway involving hydroxyl radicals ($\cdot\text{OH}$) from H_2^{18}O molecules, which were the source of ^{18}O in the phenol produced (Scheme 1). The slight decrease in the percentage of ^{18}O -labeled phenol during the reaction was probably due to the increased amount of H_2^{16}O molecules, which were generated directly by four-electron reduction of $^{16}\text{O}_2$ or indirectly by catalytic decomposition of $\text{H}_2^{16}\text{O}_2$ on Pt ; the H_2^{16}O molecules produced subsequently were used as the source of O atoms for phenol through formation of $\cdot\text{OH}$ radicals. As shown in Fig. 4, the reaction in the unlabeled H_2^{16}O solvent containing labeled $^{18}\text{O}_2$ molecules resulted in preferential production of unlabeled phenol molecules (*ca.* 95% at 15 min and 90% at 8 h). When the reaction was conducted in H_2^{16}O - H_2^{18}O (1:1) containing unlabeled $^{16}\text{O}_2$, the percentage of ^{18}O -labeled phenol was slightly less than 50% throughout the reaction (Fig. S6;† Table 4, entry 7).

These findings confirm the preferential introduction of O atoms from H_2O on the $\text{Pt}/\text{WO}_3\text{-K}$ photocatalyst. Other Pt/WO_3 photocatalysts also preferentially generated phenol that contained O atoms originating from H_2O molecules (Fig. S7 and S8;† Table 4, entries 2, 3, 10, and 11), indicating that phenol production on Pt/WO_3 proceeded through the $\cdot\text{OH}$ generation from H_2O (Scheme 1). As shown in Fig. S9,† phenol production on $\text{Pt}/\text{WO}_3\text{-K}$ was drastically suppressed by addition of a small amount of 2-propanol (188 μmol , 10 times greater than the concentration of benzene), which is an efficient $\cdot\text{OH}$ scavenger. This adds additional evidence for the reaction scheme involving $\cdot\text{OH}$ radicals.

In contrast, the Pt/TiO_2 system produced appreciable amounts of phenol containing O atoms originating from O_2 , along with others derived from H_2O , indicating that phenol production proceeded through a reaction pathway involving O_2 molecules (Scheme 2) in parallel with a pathway involving

Table 4 Direct hydroxylation of benzene in H_2^{18}O in the presence of $^{16}\text{O}_2^a$

Entry	Photocatalyst	Reaction conditions	Content of labeled phenol (%) (amount of phenol produced/ μmol)	
			15 min	8 h
1	$\text{Pt}/\text{WO}_3\text{-K}$	$^{16}\text{O}_2$, H_2^{18}O	94.7 (2.2)	91.1 (14.4)
2	$\text{Pt}/\text{WO}_3\text{-Y}$	$^{16}\text{O}_2$, H_2^{18}O	92.7 (1.0)	88.6 (11.9)
3	$\text{Pt}/\text{TiO}_3\text{-S}$	$^{16}\text{O}_2$, H_2^{18}O	92.5 (1.7)	88.9 (12.6)
4	$\text{Pt}/\text{TiO}_2\text{-P}$	$^{16}\text{O}_2$, H_2^{18}O	66.8 (0.8)	34.5 (6.1)
5	$\text{Pt}/\text{TiO}_2\text{-A}$	$^{16}\text{O}_2$, H_2^{18}O	76.6 (0.3)	68.2 (6.5)
6	$\text{Pt}/\text{TiO}_2\text{-R}$	$^{16}\text{O}_2$, H_2^{18}O	74.5 (0.1)	47.3 (1.2)
7	$\text{Pt}/\text{WO}_3\text{-K}$	$^{16}\text{O}_2$, H_2^{16}O : H_2^{18}O = 1:1	46.3 (1.2)	43.9 (14.9)
8	$\text{Pt}/\text{TiO}_2\text{-P}$	$^{16}\text{O}_2$, H_2^{16}O : H_2^{18}O = 1:1	31.6 (0.4)	16.7 (5.9)
9	$\text{Pt}/\text{WO}_3\text{-K}$	$^{18}\text{O}_2$, H_2^{16}O	4.6 (1.6)	9.9 (16.3)
10	$\text{Pt}/\text{WO}_3\text{-Y}$	$^{18}\text{O}_2$, H_2^{16}O	6.9 (1.4)	8.6 (13.2)
11	$\text{Pt}/\text{WO}_3\text{-S}$	$^{18}\text{O}_2$, H_2^{16}O	6.7 (1.6)	10.4 (14.6)
12	$\text{Pt}/\text{TiO}_2\text{-P}$	$^{18}\text{O}_2$, H_2^{16}O	35.7 (0.4)	60.4 (5.3)
13	$\text{Pt}/\text{TiO}_2\text{-A}$	$^{18}\text{O}_2$, H_2^{16}O	18.2 (0.5)	27.7 (9.7)
14	$\text{Pt}/\text{TiO}_2\text{-R}$	$^{18}\text{O}_2$, H_2^{16}O	25.8 (0.1)	53.2 (1.5)

^a Initial concentration of benzene: 500 μmol , amount of solvent: 1.0 mL, light source: 300 W Xe lamp ($300 < \lambda < 500 \text{ nm}$).

H₂O (Scheme 1). For example, photoirradiation of Pt/TiO₂-P in H₂¹⁸O with ¹⁶O₂ yielded a significant percentage of unlabeled phenol (*ca.* 33% at 15 min); the percentage was less than that of labeled phenol (Fig. 3; Table 4, entry 4). Interestingly, the percentage of unlabeled phenol increased with irradiation time (*ca.* 65% at 8 h), indicating that the contribution of the reaction pathway involving O₂ molecules becomes more dominant as the reaction progressed. Reaction in H₂¹⁶O with labeled ¹⁸O₂ also yielded a mixture of phenol molecules containing ¹⁶O or ¹⁸O (Fig. 4; Table 4, entry 12), in which the percentage of ¹⁸O-labeled phenol molecules increased from 36 to 60% as the reaction proceeded. Phenol production on Pt/TiO₂-P was suppressed slightly by addition of 2-propanol, an 'OH scavenger (Fig. S9†). Thus, phenol production on Pt/TiO₂-P proceeded simultaneously *via* two different pathways (Schemes 1 and 2), while the contribution of the pathway involving O₂ gradually becomes dominant after prolonged irradiation time. Other Pt/TiO₂ photocatalysts, regardless of crystal phase (anatase or rutile), also produced a significant percentage of phenol molecules containing O atoms originating from O₂ (Fig. 3, 4, S6, and S7†; Table 4, entries 5, 6, 13, and 14), while the change in the percentage of ¹⁸O-labeled phenol during the reaction differed significantly between Pt/TiO₂-A and Pt/TiO₂-R.

These results revealed that the Pt/WO₃ and Pt/TiO₂ systems possessed different reactivity toward oxidations as well as toward reductions. The holes generated on Pt/WO₃ photocatalysts reacted primarily with H₂O molecules, even in the presence of benzene in aqueous solution, selectively generating 'OH radicals that subsequently reacted with benzene to produce phenol. However, a portion of the holes generated on Pt/TiO₂ photocatalysts reacted directly with benzene molecules adsorbed on the TiO₂ surfaces, not only with H₂O, to generate cationic radical benzene species, which subsequently reacted with O₂ (or 'O₂⁻) and protons to produce phenol.

3.4. Reaction mechanisms for phenol production on Pt/WO₃ and Pt/TiO₂

The holes generated in WO₃ and TiO₂ demonstrate distinctly different reactivity toward hydroxylation and oxidation of benzene in water. Since the oxidative potentials of the holes generated in WO₃ and TiO₂ are essentially the same due to similarities in their valence band maxima,^{45,46} the different levels of reactivity for oxidation were likely due to the different adsorption states of benzene molecules on the surface of the photocatalyst in water. The adsorption state of benzene molecules from the gas phase onto the surface of the photocatalyst was investigated using FT-IR, while it is an indirect method for investigating the adsorbed states of benzene in aqueous solutions. The spectra before adsorption of benzene on WO₃-K (10 m² g⁻¹) and TiO₂-A (10 m² g⁻¹) were subtracted from the corresponding spectra after adsorption. The spectrum of benzene in the gas phase is also shown for comparison. As shown in Fig. S10†, only weak peaks corresponding to adsorbed benzene molecules were observed on

the WO₃-K sample at wavenumbers similar to those of benzene molecules in the gas phase, indicating that only a small number of benzene molecules were adsorbed physically on the surface of WO₃-K particles. In contrast, intense IR bands corresponding to benzene molecules adsorbed on TiO₂-A were observed at wavenumbers (1440–1540 cm⁻¹) slightly lower than those of benzene molecules in the gas phase. In addition, the IR band derived from surface hydroxyl groups of TiO₂-A, originally observed at approximately 3500–3800 cm⁻¹, decreased after benzene adsorption. This result indicated that the benzene molecules were strongly adsorbed on the TiO₂-A surface through interactions with surface hydroxyl groups, whereas benzene molecules were only physically adsorbed onto the WO₃ surface through weak interactions.

The results shown above led to the proposed reaction mechanism for direct hydroxylation of benzene to phenol in the Pt/WO₃ and Pt/TiO₂ systems as illustrated in Fig. 5. Since only a small amount of benzene molecules were physically adsorbed on the WO₃ surface, the photo-generated holes in the WO₃ photocatalyst react primarily with H₂O molecules, even in the presence of benzene molecules in aqueous solution, yielding 'OH radicals that subsequently react with benzene to produce phenol with high selectivity. At the same time, the photoexcited electrons on Pt/WO₃ photocatalysts react with molecular O₂ to generate mainly H₂O₂ on the Pt cocatalyst. The H₂O₂ generated is readily decomposed into H₂O and O₂ on the Pt cocatalyst and therefore has little impact on the hydroxylation and oxidation of benzene. In contrast, a considerable number of holes generated on Pt/TiO₂ photocatalysts react directly with benzene molecules that are strongly adsorbed on the surface *via* interactions with surface hydroxyl groups, generating cationic radical benzene species. These radicals subsequently react with O₂ (or 'O₂⁻) to give peroxy radicals that then reductively react with photoexcited electrons and protons to produce phenol. Since these peroxy radicals are generally unstable and spontaneously decompose, the formation of peroxy radicals might be a reason for the

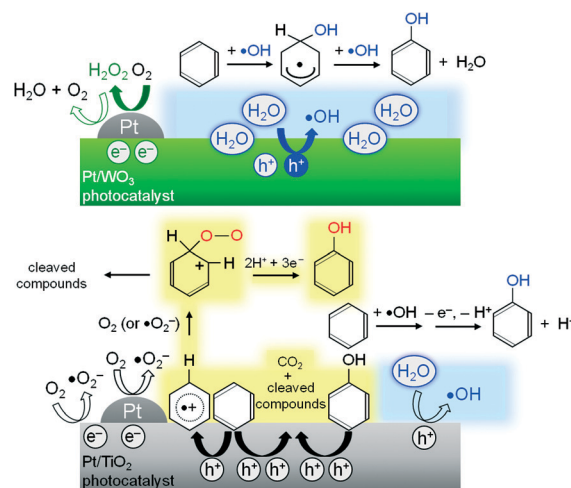


Fig. 5 Proposed reaction mechanisms for phenol production over Pt/WO₃ and Pt/TiO₂ photocatalysts.

low selectivity of TiO_2 for phenol. The adsorption of benzene molecules on the surface of TiO_2 undoubtedly increases the possibility of direct oxidation of benzene into cleaved intermediates leading to CO_2 as the final product due to the holes. This direct decomposition pathway is supported by the noticeable production of CO_2 in the initial period of photoirradiation on $\text{Pt/TiO}_2\text{-P}$ as seen in Fig. 1. Additionally, the photoexcited electrons on TiO_2 reduce O_2 into radical species such as $\cdot\text{O}_2^-$ or $\cdot\text{HO}_2$, which subsequently contribute to the oxidative decomposition of benzene and its intermediates. Both the direct oxidation of substrates (e.g., phenol) on the TiO_2 surface and the oxidation by oxygen radical species are the main reasons for reduced phenol selectivity on TiO_2 . In contrast, these two oxidation pathways are inhibited by the WO_3 system, enabling the Pt/WO_3 photocatalysts to produce phenol with high selectivity in the presence of H_2O and O_2 .

The main property of Pt/WO_3 photocatalysts that enables highly selective phenol production is the selective generation of $\cdot\text{OH}$ radicals, even in the presence of organic substances such as benzene in water. When reaction on Pt/WO_3 was initiated with 10-fold greater concentration of benzene (25 mmol L^{-1}), the amount of phenol produced only increased by ca. 16% (see Fig. S11†). Note that the results of ^{18}O -labeled reactions with a much higher concentration of benzene (500 mmol L^{-1}) indicated the preferential oxidation of water molecules on Pt/WO_3 photocatalysts. These results confirmed that the surface of WO_3 has properties that promote preferential oxidation of water molecules, even in the presence of significantly high concentration of benzene molecules, generating $\cdot\text{OH}$ radicals that are effective for selective phenol synthesis.

The specific surface area and the difference in the density of hydroxyl groups on the sample surface were considered as reasons for the differences in properties between WO_3 and TiO_2 for adsorption of benzene and its intermediates. However, the $\text{Pt/WO}_3\text{-K}$ and the $\text{Pt/TiO}_2\text{-A}$ samples, which have similar surface areas (ca. $10\text{ m}^2\text{ g}^{-1}$), had different reactivities. A series of WO_3 samples with different densities of hydroxyl groups as well as the surface areas was prepared by calcination of tungstic acid at various temperatures (XRD patterns: Fig. S12;† IR spectra: Fig. S13†) and employed as photocatalysts in the reactions with isotopically labeled $^{18}\text{O}_2$. As shown in Table S1,† the percentage of labeled phenol produced by each sample was similar, indicating that the density of surface hydroxyl groups is not the main cause of reactivity differences between WO_3 and TiO_2 systems for the oxidative process. Although the dominant property enabling the WO_3 system to produce phenol with high selectivity remains unclear and needs clarification, the unique properties of WO_3 photocatalysts for achieving highly selective phenol production in the presence of molecular O_2 probably promote practically useful organic syntheses using photocatalysis.

4. Conclusions

The highly selective phenol synthesis directly from benzene was demonstrated using Pt-loaded WO_3 photocatalysts in

water containing molecular oxygen. Results revealed that the surface of WO_3 , which is different from that of conventional TiO_2 , enables preferential oxidation of water molecules even in the presence of considerably high concentration of benzene molecules in water, to selectively generate $\cdot\text{OH}$ radicals that promote selective phenol production. This finding indicates that the $\cdot\text{OH}$ radicals can be continuously generated by simple photoirradiation (utilizing visible light) of Pt/WO_3 photocatalysts in water in the presence of O_2 ; the $\cdot\text{OH}$ radicals generated can then be used for organic synthetic reactions in water if the reactant possesses low affinity toward the surface of WO_3 . Both the efficiency and selectivity in the present system will be improved when the nature and the reaction mechanism of the WO_3 photocatalyst is better understood. The present study demonstrated the possibility of environmentally benign photocatalytic processes with potential for reducing energy consumption of fine chemical production by harnessing the energy of artificial or natural light.

Acknowledgements

This work was financially supported by the JSPS-NEXT program. The authors are also indebted to the technical division of Catalysis Research Center for their help in building the experimental equipment.

Notes and references

- 1 M. Fujihira, Y. Satoh and T. Osa, *Nature*, 1981, 293, 206.
- 2 M.-R. Hoffmann, S.-T. Martin, W.-Y. Choi and D.-W. Bahnemann, *Chem. Rev.*, 1995, 95, 69.
- 3 V. Augugliaro and L. Palmisano, *ChemSusChem*, 2010, 3, 1135.
- 4 C.-D. Jaeger and A.-J. Bard, *J. Phys. Chem.*, 1979, 83, 3146.
- 5 H. Noda, K. Oikawa and H. Kamada, *Bull. Chem. Soc. Jpn.*, 1992, 65, 2505.
- 6 L. Sun and J.-R. Bolton, *J. Phys. Chem.*, 1996, 100, 4127.
- 7 K. Ishibashi, A. Fujishima, T. Watanabe and K. Hashimoto, *Electrochem. Commun.*, 2000, 2, 207.
- 8 H. Czili and A. Horvath, *Appl. Catal., B*, 2008, 81, 295.
- 9 D.-F. Ollis, C.-J. Hsiao, L. Budiman and C.-L. Lee, *J. Catal.*, 1984, 88, 89.
- 10 Y. Sun and J.-J. Pignatello, *Environ. Sci. Technol.*, 1995, 29, 2065.
- 11 H. Einaga, S. Futamura and T. Ibusuki, *Appl. Catal., B*, 2002, 38, 215.
- 12 A. Fujishima, T.-N. Rao and D.-A. Tryk, *J. Photochem. Photobiol., C*, 2000, 1, 1.
- 13 R. Asahi, T. Morikawa, K. Aoki and Y. Taga, *Science*, 2001, 293, 269.
- 14 T. Ohno, K. Sarukawa and M. Matsumura, *New J. Chem.*, 2002, 26, 1167.
- 15 R. Inaba, T. Fukahori and M. Hamamoto, *J. Mol. Catal. A: Chem.*, 2006, 260, 247.
- 16 T. Morikawa, Y. Irokawa and T. Ohwaki, *Appl. Catal., A*, 2008, 314, 123.

- 17 H. Irie, K. Kamiya, T. Shibnuma, S. Miura, Donald A. Tryk, T. Yokoyama and K. Hashimoto, *J. Phys. Chem. C*, 2009, **113**, 10761.
- 18 O.-O. P. Mahaney, N. Murakami, R. Abe and B. Ohtani, *Chem. Lett.*, 2008, **37**, 216.
- 19 G. Palmisano, V. Augugliaro, M. Pagliaro and L. Palmisano, *Chem. Commun.*, 2007, 3425.
- 20 M. Zhang, Q. Wang, C. Chen, L. Zang, W. Ma and J. Zhao, *Angew. Chem., Int. Ed.*, 2009, **48**, 6081.
- 21 G. Zhang, J. Yi, J. Shim, J. Lee and W. Choi, *Appl. Catal., B*, 2011, **102**, 132.
- 22 T. D. Bui, A. Kimura, S. Ikeda and M. Matsumura, *Appl. Catal., B*, 2010, **94**, 186.
- 23 R. Dietz, A.-E. J. Forno, B.-E. Larcombe and M.-E. Peover, *J. Chem. Soc. B*, 1970, 816.
- 24 M.-J. Gibian, D.-T. Sawyer, T. Ungermann, R. Tangpoonpholivat and M.-M. Morrison, *J. Am. Chem. Soc.*, 1979, **101**, 640.
- 25 D.-T. Sawyer, *Acc. Chem. Res.*, 1981, **14**, 393.
- 26 M.-A. Fox, *Acc. Chem. Res.*, 1983, **16**, 314.
- 27 J. Schwitzgebel, J.-G. Ekerdt, H. Gerischer and A. Heller, *J. Phys. Chem.*, 1995, **99**, 5633.
- 28 Y. Ohko, D.-A. Tryk, K. Hashimoto and A. Fujishima, *J. Phys. Chem. B*, 1998, **102**, 2699.
- 29 H. Lee and W. Choi, *Environ. Sci. Technol.*, 2002, **36**, 3872.
- 30 Y. Li, J. Niu, L. Yin, W. Wang, Y. Bao, J. Chen and Y. Duan, *J. Environ. Sci.*, 2011, **23**, 1911.
- 31 Y. Shiraishi, Y. Sugano and T. Hirai, *Angew. Chem., Int. Ed.*, 2010, **49**, 1656.
- 32 H. Yoshida, H. Yuzawa, M. Aoki and T. Hattori, *Chem. Commun.*, 2008, 4634.
- 33 H. Yuzawa, M. Aoki, K. Otake, T. Hattori, H. Itoh and H. Yoshida, *J. Phys. Chem. C*, 2012, **116**, 25376.
- 34 B. Pal, S. Ikeda, H. Kominami and B. Ohtani, *J. Catal.*, 2003, **217**, 152.
- 35 R. Abe, H. Takami, N. Murakami and B. Ohtani, *J. Am. Chem. Soc.*, 2008, **130**, 7780.
- 36 O. Tomita, R. Abe and B. Ohtani, *Chem. Lett.*, 2011, **40**, 1405.
- 37 C. Kormann, D.-W. Bahrenemann and M.-R. Hoffmann, *Environ. Sci. Technol.*, 1988, **22**, 798.
- 38 D.-S. Arnold', C.-A. Plank, E.-E. Erickson and F.-P. Pike, *J. Chem. Eng. Data*, 1958, **3**, 253.
- 39 L.-A. Lyon and J.-T. Hupp, *J. Phys. Chem. B*, 1999, **103**, 4623.
- 40 C. Walling, *Acc. Chem. Res.*, 1975, **8**, 125.
- 41 W. Matthews, *J. Chem. Soc., Faraday Trans. 1*, 1984, **80**, 457.
- 42 S. Goldstein, G. Czapski and J. Rabani, *J. Phys. Chem.*, 1994, **98**, 6586.
- 43 T.-D. Bui, A. Kimura, S. Ikeda and M. Matsumura, *J. Am. Chem. Soc.*, 2010, **132**, 8453.
- 44 Y. Li, B. Wen, C. Yu, C. Chen, H. Ji, W. Ma and J. Zhao, *Chem. – Eur. J.*, 2012, **18**, 2030.
- 45 D.-E. Scaife, *Sol. Energy*, 1980, **25**, 41.
- 46 M. Miyauchi, A. Nakajima, T. Watanabe and K. Hashimoto, *Chem. Mater.*, 2002, **14**, 4714.